Engineering Science and Technology, an International Journal 23 (2020) 801–811

HOSTED BY

Contents lists available at ScienceDirect

Engineering Science and Technology, an International Journal

journal homepage: www.elsevier.com/locate/jestch

Full Length Article

Performance evaluation of the submerged abrasive water jet turning process for improving machinability of castamide

Salem A. Basher Ibrahim [a], Seyma Korkmaz [a], M. Huseyin Cetin [a,*], Fuat Kartal [b]

[a] Karabuk University, Engineering Faculty, Mechanical Engineering Department, Karabuk 78050, Turkey
[b] Kastamonu University, Engineering and Architecture Faculty, Mechanical Engineering Department, Kastamonu 37150, Turkey

ARTICLE INFO

Article history:
Received 19 January 2020
Revised 18 May 2020
Accepted 14 June 2020
Available online 25 June 2020

Keywords:
Submerged turning
Abrasive water jet
Castamide
TOPSIS
VIKOR

ABSTRACT

In this study, the submerged abrasive water jet turning (AWJT) system was used for improving machinability of castamide material and process parameters have been investigated comprehensively. Optimum parameters were determined as to minimize the surface roughness and maximize the material removal rate in the submerged turning process of castamide. 3-level traverse speed (TS), abrasive flow rate (AFR) and spindle speed (SS) were taken as the input parameters, and the experimental design was made as a full factorial design. The effect ratios of the input parameters were analyzed statistically by ANOVA and graphical methods, and their interactions were examined by 3D surface images. Optimum test condition was determined by TOPSIS and VIKOR methods. Experimental results were compared with conventional abrasive water jet process. In addition, regression equations were obtained for the explanation of the experimental results mathematically to show the relationships between the variables. According to the experimental results, submerged AWJT increased the surface roughness of castamide material by 15% compared to conventional AWJT and decreased the metal removal rate by 5.22%. ANOVA results showed that the traverse speed is the most effective parameter on the machinability of castamide. Traverse speed was found to be 83.11% effective on surface roughness and 85.56% on material removal rate. According to TOPSIS and VIKOR optimization results, 40 mm/min TS, 310 g /min AFR and 300 rpm SS values were determined as the optimum test conditions.

1. Introduction

In the abrasive water jet (AWJ) process, which is a non-traditional material processing technology, engineering materials with high hardness and brittleness can be processed with high precision by erosive effect [1–7]. Thanks to the high pressure created in the AWJ process, ceramics, glass, rock, high hardness steels (>60 HRC) and composites can be processed [8–14]. In the water jet process, a rigid cutting can be performed by adding hard abrasive particles into the water jet. Also, since there is no thermal effect in the process, distortion, microstructure and mechanical softening-based problems are not observed. No thermal effect is vital to increase the machinability of polymer materials. The disadvantages of the AWJ process are high noise generation (>100 dB), pressure-dependent water splash and conical edge formation over the kerf [15,16].

Generation of high heat and high operating temperatures during machining of engineering materials are inevitable. The generated energy by the friction between the workpiece and the cutting tool and the separation of atomic bonds during plastic deformation are the main reasons of the increasing temperature. Metallic materials have a high thermal conductivity coefficient compared to other engineering materials, so they are less affected by thermal deformation. However, in polymer materials, undesirable manufacturing problems arise due to high temperature such as distortion, increase in surface roughness, material plastering, build-up edge [17–20]. By optimizing the process parameters during the machining process of polymer materials, these faults can be minimized [21]. However, optimizing parameters is not enough to improve surface quality as a high amount of heat is generated during the machining applications due to high speed and load. Using cutting fluids is essential to remove heat from the workpiece. However, the negative effects of mineral and semi-synthetic cutting fluids on the environment and human health limit the use of them [22–24]. The use of vegetable-based cooling fluids in machining is limited since they have a low tribological performance at high temperatures due to their low thermo-oxidation resistance

* Corresponding author.
E-mail addresses: hcetin@karabuk.edu.tr (M.H. Cetin), fkartal@kastamonu.edu.tr (F. Kartal).
Peer review under responsibility of Karabuk University.

https://doi.org/10.1016/j.jestch.2020.06.009
2215-0986/

[25,26]. For these reasons, it is necessary to use a process without heat generation in order to increase the machinability of the polymer materials. The water-jet process, in which cutting can be carried out without increasing the temperature, is very useful for increasing the machinability of polymer materials and improving the surface quality [13,27–30]. Kartal et al. [31], investigated the optimum parameters for minimum surface roughness (Ra) and maximum material removal rate (MRR) in the turning of low-density polyethylene material by experimental and statistical methods, and concluded that AWJ method is an effective method for machining polymers. In this study, three levels were determined for traverse speed (TS), abrasive flow rate (AFR) and spindle speed (SS), and a full factorial experimental design was established. According to the analysis results, 5 mm/min TS, 350 g/min AFR and 2500 min^{-1} SS were obtained as optimum parameters for minimum Ra (1.67 μm) and maximum MRR (14072.02 mm^3/min).

Eliminating the thermal effects during the AWJ machining of the polymer materials, machinability can be significantly improved [32]. However, there are problems associated with surface quality and ergonomics [33]. Surface roughness is highly effective in determining the fatigue life of the materials operating under dynamic loads. Low surface quality in the AWJT process is related to the explosion behavior of the water jet after it exits the nozzle. Due to the pressure change, the water jet is scattered along with the abrasive particles. Due to this scattering behavior, the rigidity of the cutting jet contacting the material decreases and the surface quality of the material is deteriorated. Furthermore, the AWJT process produces noise and splash problems induced by high pressure. High-pressure AWJ produces noise at an unacceptable level (~110 dB) for workers' health [34,35]. To solve problems of surface quality and sound ergonomics, the scattering behavior in the jet nozzle should be controlled.

In this study, it has been hypothesized that the problems above can be solved by operating the jet nozzle at submerged conditions under hydrostatic pressure. Therefore, a submerged AWJT system was used and machinability of castamide material was investigated as the novelty of the study. The aim of underwater turning is to ensure that the water jet under hydrostatic pressure is contacted to the workpiece material with a minimum scattering behavior and minimizing hypersonic water jet noise. It is also important for the stability of the water jet that abrasive particles are exposed to high friction in water. This study is unique in the literature by using of the submerged AWJT apparatus for improving the machinability of castamide materials. Also, there are limited studies on the investigation of the machinability of polymer materials using submerged AWJT process. Castamide material was preferred as the test material due to its importance in engineering applications and its extensive use in machine design [36]. The experiments were carried out according to the full factorial design, and the experimental results were evaluated and optimized using statistical methods (variance and regression analyses, TOPSIS and VIKOR).

2. Material and method

2.1. Characterization of experimental material

Mechanical, thermal and physical properties of the castamide material used in the study are given in Table 1. Castamide is one of the most preferred engineering plastics due to its ~85 MPa strength, 1.10 g/cm^3 density and high hardness (Shore D: 84). Also, castamide is used in bearings with high stability in wear conditions [36]. For this reason, it is of industrial importance to increase the machinability of castamide material which is directly related to surface quality. However, due to the high temperature during the conventional machining process, the castamide material melts, the surface form of the material deteriorates, and the surface roughness increases. In addition, the melted plastic material smears back onto the material surface by the cutting tool which makes it hard to obtain an acceptable surface quality (Fig. 1). In order to increase the machinability of castamide, methods not producing heat effect are required. AWJT is one of such machining processes and can be used to improve the machinability of castamide

Table 1
Engineering properties of cast-polyamide [36].

Property	*Unit*	*Value*
Density	g/cm^3	1.15
Water absorption	%	6–7
Tensile strength	MPa	90
Modulus of elasticity	GPa	4
Tensile elongation	%	>20
Impact strength (Izod, notched)	kJ/m^2	5.6
Hardness (Shore D)	Shore D	84
Melting temperature	°C	220
Thermal elongation	1/K.10^5	8–9

2.2. Introduction of submerged abrasive water jet system

In this study, a submerged AWJ turning assembly was used to minimize the problems above (Fig. 2). The AWJ lathe is made by combining a conventional lathe with a water-jet machine. In the assembly, the abrasive-added water jet works as a cutting tool and the lathe apparatus rotates the workpiece. Submerged assembly passes the abrasive jet from the high-pressure zone to the hydrostatic pressure zone and thus minimize the expansion of the jet producing a better cutting profile (Fig. 3).

Submerged AWJT experimental setup uses a 0.37 kW electric motor and ATV 12 380 V–220 V control card for the motor speed control which can turn the motor at a constant speed and torque at the desired direction. Turning mechanism was constructed using a belt and pulley and key coupling. A surface hardened chrome shaft is used as a spindle. The roller bearing is used as bearing element. In the lathe, a 100 mm diameter three-jaw chuck was used

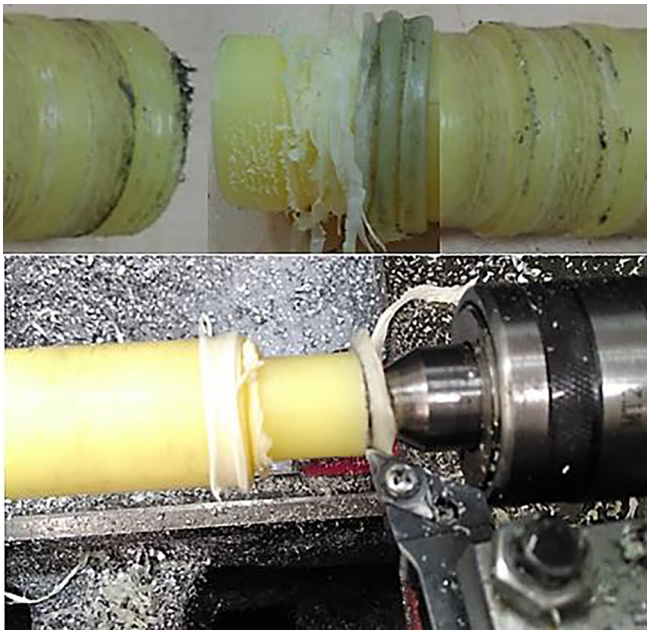

Fig. 1. Surface quality deterioration due to melt spinning.

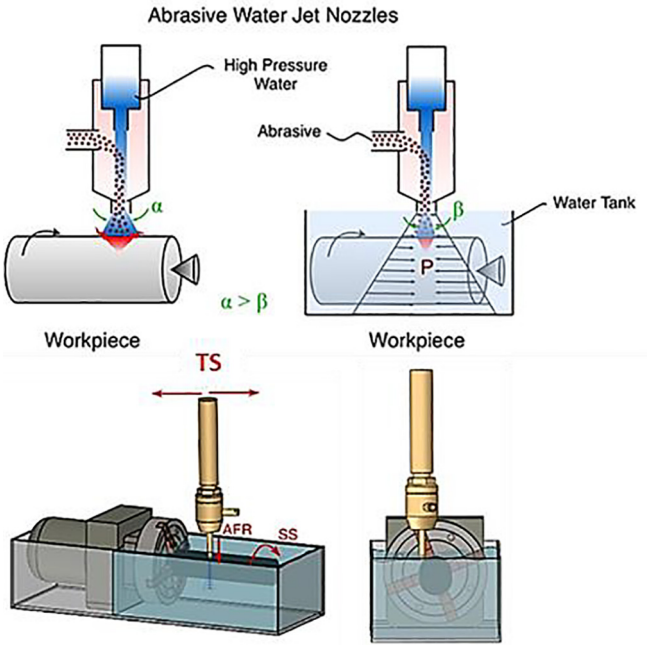

Fig. 2. Behaviour of water jet in submerged cutting conditions and 3d drawing of submerged abrasive water jet process (Perspective and front side).

Fig. 3. Submerged abrasive water jet experimental setup.

to hold the workpiece. A digital dial gauge with a precision of 0.001 mm was used to detect the deviation of the system axis. In the designed system, the axial offset value of spindle and lathe chuck was measured as 0.001 mm. SL-V 50 KMT model pump is used and the tests were conducted under 3800 bar constant pressure. For sealing mechanical and electronic equipment, liquid gasket and protective cover are used. Mineral-based garnet material of ~80 mesh size was used as an abrasive particle. Garnet material is a preferred abrasive due to its antitoxic properties and having no corrosive effect. Garnet material's SEM images are given in Fig. 4 which shows the multiple sharp-edged structures of the garner. This form enables the many contact areas with high tensile values and the material can be cut rigidly.

2.3. Experimental design

In the experiments, TS, AFR and SS values were considered as input parameters (Table 2). Parameter levels were determined

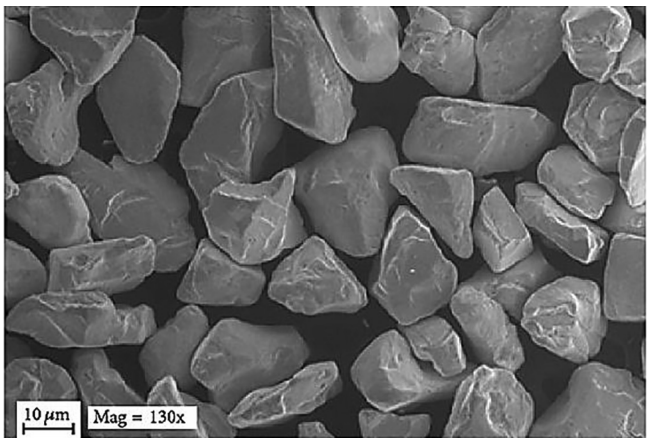

Fig. 4. SEM image of the garnet abrasive material.

based on the preliminary tests and literature review and 3 levels were determined for each parameter [32]. Surface roughness (R_a) and material removal rate (*MRR*) parameters were measured as output parameters (Table 2). The experiment was designed using full factorial design method and a total of 27 different conditions ($n^k = 3^3$) were tested. Nozzle stand-off distance parameter was kept constant at a length of 2 mm. In Fig. 5, the fixed parameter defined by nozzle stand-off distance is shown schematically. Turning was done under the condition that the nozzle tip is tangent to the workpiece and the cutting depth parameter was formed according to the scattering of the jet. In the literature, nozzle stand-off distance parameter was defined as the depth-of-cut parameter, similar to that used in conventional turning [37]. This approach is important for analytical calculations. However, in the experimental study, it was determined that different diameter values were formed in each pass due to the changes in the manufacturing parameters depending on the design of the experiment. For this reason, the MRR parameter was calculated and analyzed as the output parameter by measuring the diameter values formed after each pass. But, considering the MRR values, it can be said that the depth-of-cut is approximately 1 mm. Mitutoyo SJ-301 type desktop profilometer was used for surface roughness (R_a) measurements. The cut-off length was determined as 0.8 mm. Three measurements were done for surface roughness and the mean value is taken. To calculate the metal removal rate, the diameter of the workpiece before and after the machining is measured using a caliper, and *MRR* is calculated using Eq. (1) where, i is the test number, D_i is the diameter before the machining, D_{i+1} is the diameter after machining, and h is the machined length. Noise measurement was performed by PCE-MSM 4 (±1.4 dB accuracy) equipment. The second-order variance analysis (ANOVA) is used to analyze the experimental results and the significance levels were calculated by regression analysis. The ANOVA test provides a quantitative measurement of the effect of input parameters on the output parameters. Additionally, regression coefficient values (R-Sq and R-Sq Adj.) are important to measure the statistical significance and adequacy of the experiment setup. Depending on the experience obtained for machinability, it can be said that the regression coefficient values 80% and more are enough for the AWJT process [38]. In the evaluation of the experimental results, the minimization criterion for R_a and the maximization criterion for *MRR* were considered. The optimum test conditions were determined using TOPSIS and VIKOR methods which are known to have high reliability and ease of application among the multi-criteria decision-making methods [39–41]. For R_a and *MRR*, a weight value of 0.5 was considered. In solution Table of TOPSIS, S_i^+, S_i^- and C_i

Table 2
Experimental input and output parameters.

Input parameters	*Units*	*Level 1*	*Level 2*	*Level 3*	*Output parameters*	*Units*
Traverse speed (TS)	mm/min	40	140	240	Surface roughness (R_a)	μm
Abrasive flow rate (AFR)	g/min	110	210	310	Material removal rate (*MRR*)	mm^3/min
Spindle speed (SS)	rpm	100	200	300		

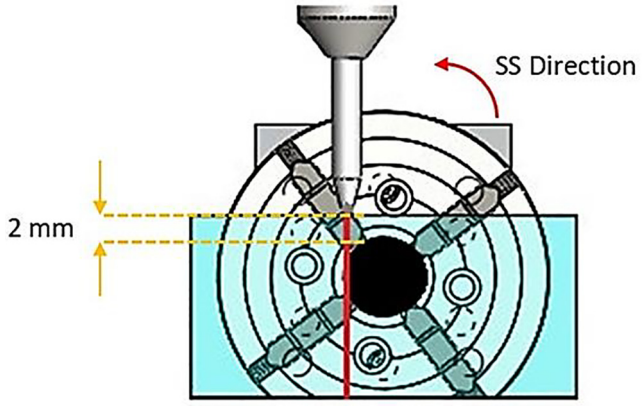

Fig. 5. Schematic of nozzle stand-off distance parameter.

Fig. 6. Process conditions of (a) Conventional AWJT and (b) Submerged AWJT.

parameters was used as optimum ideal, negative ideal and ideal parameter indicators, respectively. In solution Table of VIKOR, ΣE_i, F_i, Q_i parameters was used as first solution coefficient, second solution coefficient and ideal parameter indicators, respectively.

In the study, conventional AWJT results from the literature was used to compare the performance of the submerged AWJT process [32]. Normally, the comparison of underwater AWJT and conventional AWJT results had to be performed with the same parameters in both experiments. However, due to the resistance occurring under underwater conditions, it was not possible to reach high spindle speeds possible at the conventional method. Additionally, it was realized that sealing problem at high speeds would be a serious problem. For this reason, comparisons can be made by considering the nominal test values in both conditions.

$$MRR_i = \left(\pi.\left(D_i^2 - D_{i+1}^2\right)/4\right).h \quad (1)$$

3. Results and discussion

Noise and splashing in the conventional AWJT process is given in Fig. 6(a), and the noise and machining conditions with the submerged AWJT are given in Fig. 6(b). The sound level was reduced from 108.8 dB to 86.1 dB by the submerged method. In addition, a stable machining zone was formed by avoiding splash.

The experiments performed according to the full factorial experimental design and the obtained R_a and *MRR* values are given in Table 3 which shows that the lowest value for R_a is 1.46 μm which was achieved in the 6th test. Kartal and Yerlikaya [32], achieved a minimum of 1.73 μm roughness value in turning castamide with conventional AWJT. Results show a 15% increase in the surface quality for the submerged AWJT process. Kartal and Yerlikaya [32], achieved a maximum 212 mm^3/min MRR value which was decreased to 200.93 mm^3/min by a 5.22% decrease using submerged AWJT process (Table 3). MRR decreased due to the resistance caused by hydrostatic pressure under submerged conditions. However, according to these results, it is difficult to say that the submerged AWJT process is effective or not. According to the experiences from the AWJ process, output parameters variation up to 20% could be caused by material in-homogeneity, local disorders in jet pressure, suction-based problems and machine movement. Therefore, uncertainties up to 20% are considered to lay within an interval of AWJ uncertainty and improvement of any qualitative or quantitative parameter within this range cannot be considered as a significant one. In this situation, according to the results, it can be said that the submerged AWJT process has similar characteristics in terms of R_a and *MRR* with the conventional AWJT process. However, reducing the noise and splashing problems in the underwater AWJT process makes an important difference. For this reason, submerged AWJT is more advantageous in general comparison. In addition, the possible causes of the results obtained for R_a and *MRR* were tried to be discussed, although they are considered within the uncertainty.

The lower R_a formation in the submerged AWJT method can be explained by the expansion behavior of the water jet shown in Fig. 2. In the conventional AWJT process, water jet moves at high pressure through the nozzle [42,43], and when the water jet leaves the nozzle, it passes from a high-pressure zone to a low-pressure zone and the jet expands. Because of this behavior, the linear flow behavior of the cutting jet is deteriorated, and the stability is lost, and the pressure value gained for cutting the material is reduced due to its increased effect area. This can also be defined as a transition from laminar flow to turbulent flow. It is an expected result that as the flow behavior deteriorates, R_a value is negatively affected. In the submerged AWJT process, water jet with a huge pressure (~3800 bar) in the nozzle passes into a hydrostatic pressure area which minimizes the expansion of water jet and provides a stable cutting operation.

SEM images obtained for the conventional and submerged AWJT processes also support the results obtained for surface roughness (Fig. 7). In the conventional AWJT process, because of the expanding water jet profile, it is expected that the abrasive particles in the water jet will be dispersed and that the micro-size particles stuck into the surface of the castamide material. In the submerged AWJT process, it is expected that more controlled dissemination of abrasive particles onto the surface of the workpiece due to the reduction of the water jet expansion.

Table 3
Experimental results.

Exp. No	Input parameters			Output parameters	
	TS (mm/min)	AFR (g/min)	Spindle speed (rpm)	R_a (μm)	MRR (mm^3/min)
1	40	110	100	2.89	142.79
2	40	110	200	2.81	149.88
3	40	110	300	1.92	154.10
4	40	210	100	2.56	154.88
5	40	210	200	2.11	158.60
6	40	210	300	1.46	169.07
7	40	310	100	1.52	185.25
8	40	310	200	1.61	192.52
9	40	310	300	1.95	200.93
10	140	110	100	4.25	114.94
11	140	110	200	3.27	117.13
12	140	110	300	3.97	120.94
13	140	210	100	3.81	125.93
14	140	210	200	3.17	127.46
15	140	210	300	3.37	129.77
16	140	310	100	2.57	132.11
17	140	310	200	2.68	135.39
18	140	310	300	3.07	138.89
19	240	110	100	5.46	79.76
20	240	110	200	5.42	84.93
21	240	110	300	5.04	85.63
22	240	210	100	4.27	88.01
23	240	210	200	4.92	88.82
24	240	210	300	4.89	94.90
25	240	310	100	4.49	96.65
26	240	310	200	4.40	99.73
27	240	310	300	4.28	103.71

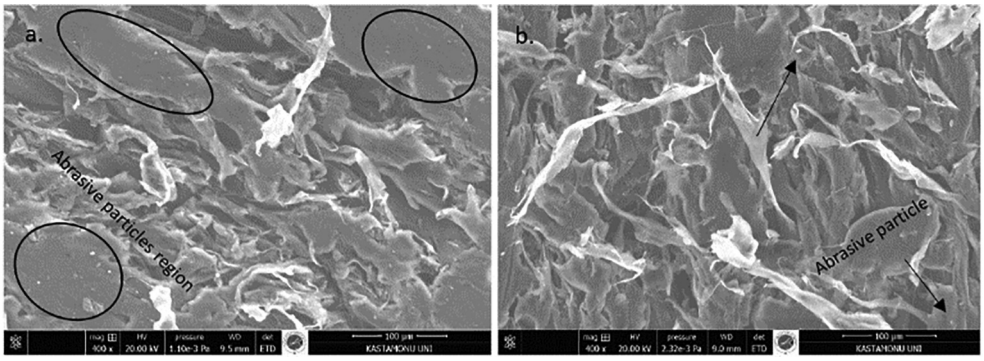

Fig. 7. Surface SEM images of (a) Conventional AWJT, (b) Submerged AWJT (In conditions of 240 mm/min TS, 110 g/min AFR and 100 rpm Spindle Speed).

In Fig. 7(a), abrasive particles concentrated on the surface are shown. Fig. 7(b) shows that there are abrasive particles only at certain locations on the surface. SEM images were obtained for experimental conditions where surface roughness is the maximum. Images show that the submerged AWJT method is successful in reducing surface roughness.

The behavior of abrasive particles in the jet is also important on the surface roughness. Abrasive particles break down significantly under high pressure. At this stage, large particles are drawn towards the slower outer part of the jet, while small particles are drawn towards the faster central part of the jet [8]. In this case, the abrasive effects of large particles decrease as they are exposed to more braking due to air friction. However, the significance of this effect should be discussed by material type. In the processing of steel materials, the effect on surface quality may decrease due to the decreasing energy. In polymer materials, even if the energy of the particles on the outer surface of the jet decreases, the outer particles will influence the material surface form due to the low strength of the polymer materials. In addition, braking abrasive particles when contacting the polymer material is important for surface quality. Particles stuck on the soft surface of polymer materials cause increased surface roughness. For this reason, the braking of particles in water instead of air and losing their energy with more friction effect is vital for reducing the surface roughness values of polymer materials. In addition, even if the braking energy underwater is too high, the pressure value of the particles will be more than enough to process the polymer material.

3.1. Effect of process parameters on R_a

The effects of process parameters were determined by ANOVA, and surface roughness results were given in Table 4. The input parameters that are most effective on R_a value are the traverse speed (83.11%) and the abrasive flow rate (10.1%). Spindle speed (0.53%) has no significant effect on R_a (Table 4). The values obtained from the F test confirm the effect ratios and agrees with the literature [44,45]. Two-way interaction of the parameters didn't make a significant change on surface roughness. According to p values in Table 4, TS ($p = 0 < 0.05$) and AFR ($p = 0.002 < 0.05$) has statistically and physically significant effect on R_a while SS

Table 4
ANOVA results for surface roughness.

Source of Variance	Degree of Freedom (DF)	Sum of Squares (SS)	Mean of Squares (MS)	F Ratio	P	Effect Rate (%)
TS	2	33.0761	16.5381	124.51	0.000	83.11
AFR	2	4.0189	2.0094	15.13	0.002	10.1
SS	2	0.2096	0.1048	0.79	0.487	0.53
TS * AFR	4	0.1356	0.0339	0.26	0.899	0.34
TS * SS	4	0.7853	0.1963	1.48	0.295	1.97
AFR * SS	4	0.5079	0.1270	0.96	0.481	1.28
Error	8	1.0626	0.1328			2.67
Total	26	39.7961				100
Significance	R-Sq = 97.33% R-Sq (adj) = 91.32%					

($p = 0.487 > 0.05$) is not significantly effective. Although the effect ratio of AFR parameter can be considered as low (10.1%), it is an important result that it has statistical and physical effect according to the p-value. The R-Sq (adj) value given in Table 4 for the surface roughness was found to be 91.32%. This ratio proves the reliability of the test system when it is equal and over 80% [38,46]. The statistical graphs obtained for the R-Sq (adj) value are given in Fig. 8. According to the normal distribution graph given in Fig. 8 (a), all experimental data are listed on the regression line. The histogram graph is given in Fig. 8(c) also shows behaviour close to the normal distribution curve (Percentage deviation is 0.15% while the standard deviation is 1.237%) [47]. The difference between the experimental graph and the actual graph can be explained by the low significance data points shown in Fig. 8(b) and (d). These points negatively affecting the significance of the experimental data are produced by some unexplained factors during the experiment such as vibration, temperature variation etc.

Fig. 9 gives the topography graphs obtained for the variation of R_a values according to the change of parameter levels. According to Fig. 9, the surface roughness increased with the parameter TS, which had an effect of 83.11% on the surface roughness. Due to the increase in the traverse speed, the nozzle waiting time required to process the castamide material will be reduced. In the AWJT process, the abrasive jet first applies a rough cutting process. Then, by increasing the waiting time of the nozzle, a finish material removal process is applied to the surface. Because of the decreased machining time due to increased TS, finish cutting process couldn't be applied which was required to achieve a low roughness value. Additionally, a spiral track is formed on the rotating workpiece depending on the linear movement of the nozzle. Increasing speed also increased the length between spiral tracks which increases the roughness. Kartal and Yerlikaya [32], found the effect ratio of TS parameter as 87.1% in conventional AWJ method. The effect of TS decreased by 4% in submerged machining conditions. Increasing TS negatively affects the R_a value. Therefore, decreasing the effect ratio of TS is an achievement for increasing machining speed.

The effect rate of AFR parameter (10.1%) was found the same as Kartal and Yerlikaya [32]. Since the water contacts the workpiece under 3800 bar pressure, the effect of AFR parameter on R_a was found the same for both conventional and submerged systems. The correlation between the change in AFR value and the surface roughness values is consistent with the literature [32]. As the AFR value increased, surface roughness values decreased (Fig. 9 (a) and (b)). With the increase of AFR, more abrasive particles contact the workpiece and better surface roughness is achieved. Due to the increased amount of abrasive, the cutting jet acts more rigidly and homogeneously on the cutting zone. It can be claimed that laminar flow can be achieved due to increased rigidity and

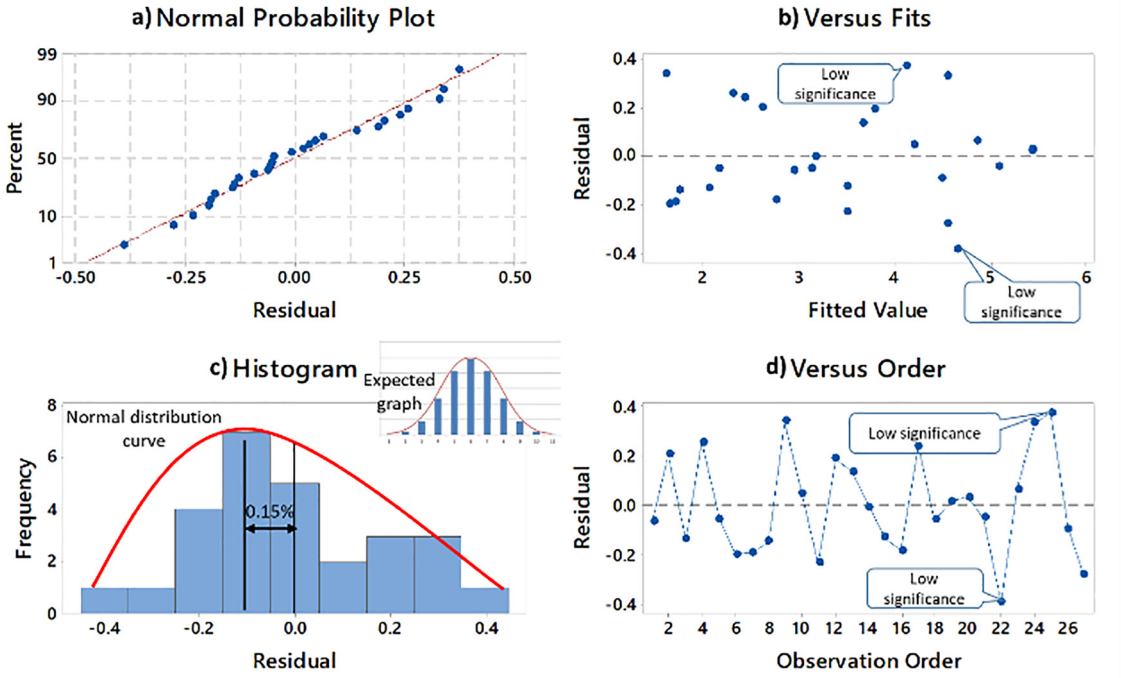

Fig. 8. Statistical graphs for the reliability of *Ra* results.

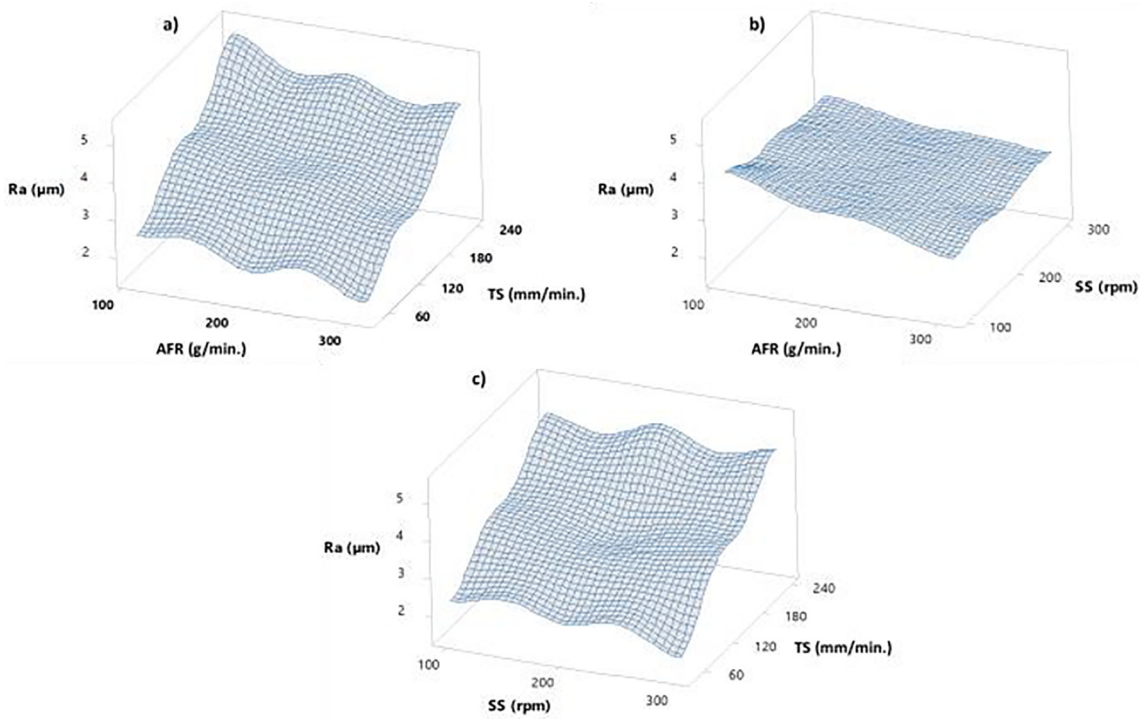

Fig. 9. Topography images for understanding the effects of process parameters on R_a.

homogeneity. Therefore, the increase in AFR ratio positively affected the surface quality.

The effect rate of the SS parameter (0.53%) decreased compared to the results of Kartal and Yerlikaya [32] (1.1%). The hydrostatic pressure in the submerged system increases the friction force on the workpiece, making the rotation difficult. Therefore, the effect of SS parameter in submerged AWJT process decreased compared to that of the conventional AWJT process. Variation of SS parameters and the surface roughness indicate no significant correlation between the parameters (Fig. 9(b) and (c)). It can be claimed that the protective water film layer formed by centrifugal forces on the workpiece prevented the interaction between SS parameter and R_a.

3.2. Effect of process parameters on material removal rate (MRR)

The effect of machining parameters on the *MRR* was determined by ANOVA method (Table 5). According to Table 5, the effect rates of machining parameters TS, AFR, SS on *MRR* were determined as 85.56%, 10.26% and 1.10%, respectively. The values obtained from the *F* test confirm the effect rates. Kartal and Yerlikaya [32] found the effect ratio of TS, AFR and SS for the conventional AWJT as 82.56%, 11.36% and 1.73%, respectively.

Based on the ANOVA results, no significant difference was found between the submerged and conventional AWJT. According to *p* values in Table 5, TS ($p = 0 < 0.05$), AFR ($p = 0 < 0.05$) and SS ($p = 0 < 0.05$) parameters has statistically and physically significant effect on MRR. Besides, the interaction of TS parameter with AFR ($p = 0 < 0.05$) and SS ($p = 0.002 < 0.05$) parameters was found to be statistically and physically important. As seen in Table 5, the R-Sq(adj) value for *MRR* was found as 99.89%. According to this value, the input parameters considered can fully explain the variation of the *MRR* parameter. The statistical graphs obtained for the R- Sq (adj) value are given in Fig. 10. According to the normal distribution graph given in Fig. 10(a), all experimental data are distributed on the regression line. The histogram graph in Fig. 10(c) shows normal distribution curve behavior (Percentage deviation is 0% while the standard deviation is 34.30%). In Fig. 10(b) and (d), the distances between the test results and the regression line are graphically given. Test data distributed homogeneously along the center axis and the normal distribution curve in the histogram confirms the significance of the test data in the 95% confidence region.

Topographic graphs representing the variation of *MRR* values according to the change of parameter levels are given in Fig. 11. According to Fig. 11(a) and (c), *MRR* value decreased by the

Table 5
ANOVA results for material removal rate (MRR).

Source of Variance	Degree of Freedom (DF)	Sum of Squares (SS)	Mean of Squares (MS)	F Ratio	P	Effect Rate (%)
TS	2	26172.6	13086.88	10079.88	0.000	85.56
AFR	2	3137.7	1568.9	1208.42	0.000	10.26
SS	2	336.3	168.2	129.53	0.000	1.10
TS * AFR	4	858.8	214.7	165.37	0.000	2.81
TS * SS	4	59.8	14.9	11.51	0.002	0.19
AFR * SS	4	13.2	3.3	2.54	0.122	0.05
Error	8	10.4	1.3			0.03
Total	26	30588.8				100
Significance	R-Sq = 99.97% R-Sq (adj) = 99.89%					

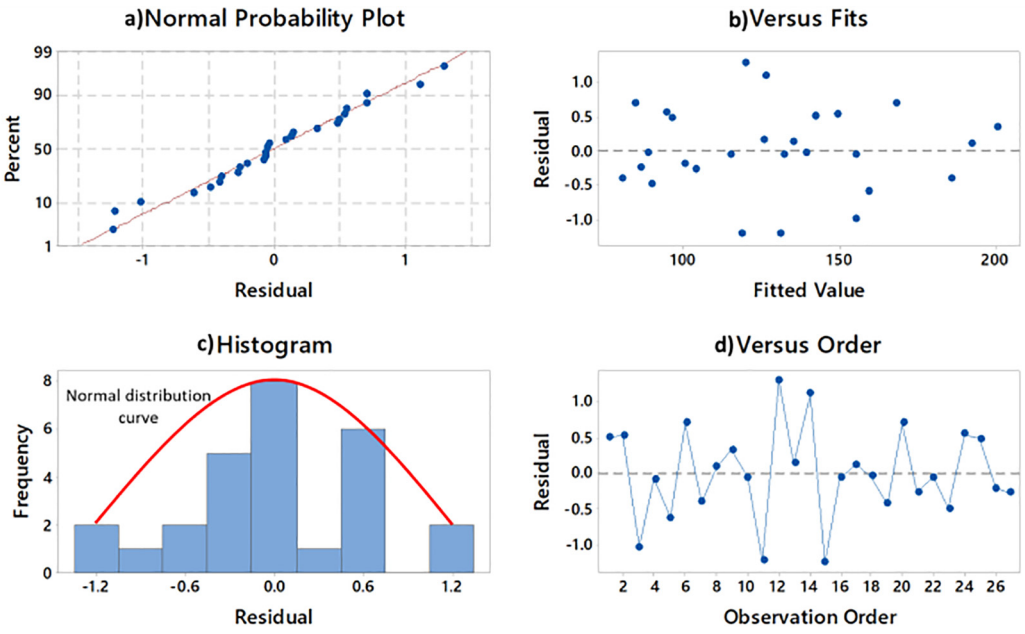

Fig. 10. Statistical graphs for the reliability of MRR results.

increasing TS parameter, which is 85.56% effective on MRR. Machining time decreases with increasing TS. Due to the shorter machining time, the contact duration between the abrasive material and the castamide was reduced and thus the *MRR* values decreased. According to Fig. 11(a) and (b), *MRR* value increased by the increasing AFR. Increasing *MRR* value can be explained by the increasing flow rate of particles contacting the castamide material. As the AFR increases, the cutting stability will increase due to increased jet rigidity. This can also be expressed as penetration to the determined depth of cut. Increased penetration enabled better material removal. Fig. 11(b) and (c) show that *MRR* didn't change by the SS parameter. TS and AFR parameters have high physical effects on MRR, and therefore the SS parameter didn't show a significant effect.

3.3. Optimization of process parameters

Optimum process parameters of submerged AWJT process are determined by TOPSIS and VIKOR methods. Minimization of R_a and maximization of *MRR* was considered as the goal functions.

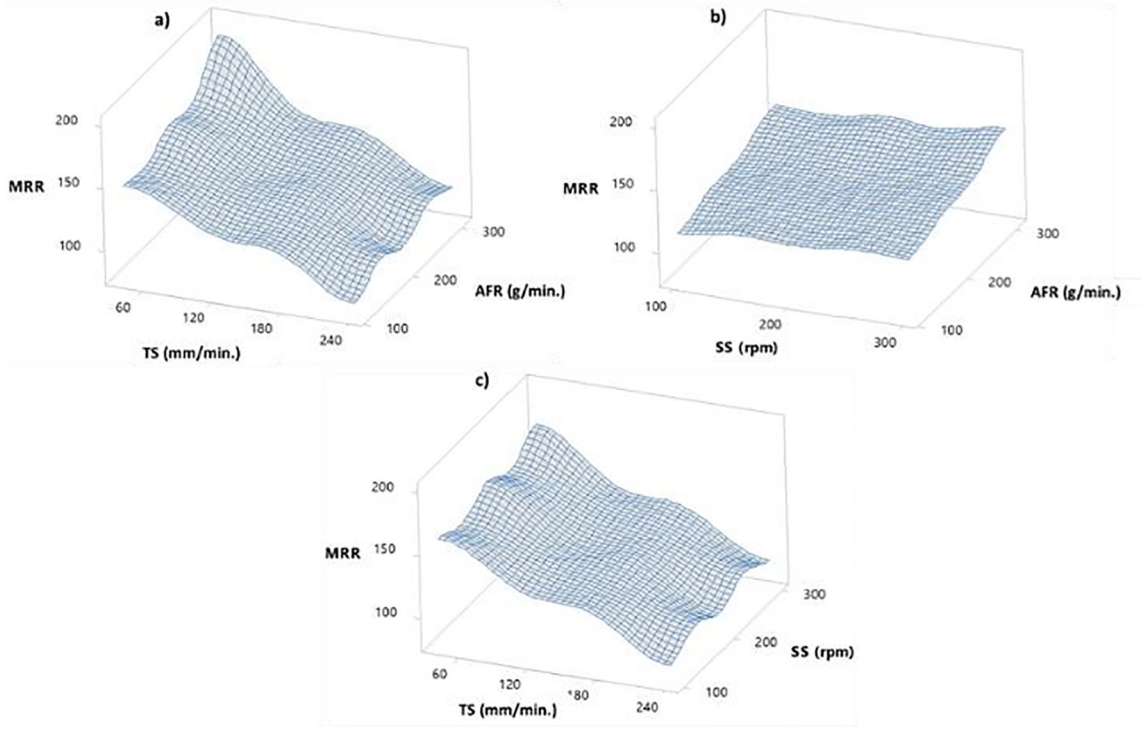

Fig. 11. Topography images for understanding the effects of process parameters on MRR.

Table 6 indicates that the optimum point in both TOPSIS and VIKOR methods is testing conditions of the number 9 (TS: 40 mm/min, the AFR is 310 g/min, SS 300 rpm). The R_a value measured in experiment 9 is 1.95 μm, and the calculated MRR is 200.93 mm^3 /min. Optimum conditions were obtained at minimum levels of TS and maximum levels of AFR and SS parameters. ANOVA and topography results agree with data obtained from optimum points. Therefore, the results obtained from TOPSIS and VIKOR methods are reliable. In addition, the same results obtained by two different methods increases reliability.

3.4. Regression analyses for obtaining empiric equations

Eq. (2) was used for the *Ra* value determined based on the experimental results. A multilinear regression analysis (Eq. (3)) was performed to predict the R_a and *MRR* [48,49]. Since the parameter changes in Figs. 9 and 11 are linear, there is no need for expressions of the equation containing second-degree polynomials and interactions. Regression analysis was applied to experimental results to develop mathematical equations explaining the relationships between variables (Eqs. (4) and (5)). Equations can be used for estimation and reliability tests. The TS, AFR and SS parameters were considered as independent variables, while R_a and *MRR* parameters were considered as dependent variables in the modeling studies. The equations were obtained as linear without interactions; i.e. less independent parameter was used for practical usage of equations [48,49].

$$R_a = \frac{1}{L}\int_0^L |y(x)||dx| \tag{2}$$

$$R_a = \beta_0 + \sum_{i=1}^{k}\beta_i X_i + \sum_{i=1}^{k}\beta_{ii}X_i^2 + \sum\sum_{i<j}\beta_{ij}X_iX_j + \varepsilon_i \tag{3}$$

$$Ra(\mu m) = 2.715 + 13x10^{-3}TS - 4x10^{-3}AFR - 1x10^{-3}SS \tag{4}$$

$$MRR = 145.92 - 38.1\times10^{-2}TS + 13\times10^{-2}AFR + 43\times10^{-3}SS \tag{5}$$

3.5. Confirmation tests

Confirmation tests were performed for optimum point and regression equations obtained from TOPSIS and VIKOR algorithm. In addition to the optimum value, two randomly determined test conditions were also considered to improve reliability. Error-values were calculated according to Eq. (6). According to the confirmation tests in Table 7, a maximum of 13.07% and 8.49% error is determined for the R_a and MRR respectively between the estimated value and the actual results. In addition, the regression equations were applied to all parameters in Table 3, and it was determined that the mean error is 9.99% for the *Ra* value and 3.72% for the *MRR* value. Cetin et al. [38] argue that 20% and less error indicates acceptable reliability. However, it is not correct to generalize these equations for the submerged AWJT process. It is stated in the literature that these equations have limited validity [50–53]. An underwater AWJT process must be analyzed analytically to find general equations. In the literature, there are analytical equations developed for speed, diameter and manufacturing angles [1,2,6,8,12,54–56]. However, analytical models developed for R_a and *MRR* parameters are not sufficient. On the other hand, there is an analytical model used in conventional turning for surface roughness. In Eq. (7), f represents the tool feed rate, and r is the cutting tool radius. However, the usability of this equation for submerged AWJT is not possible. Although the feed rate and *TS* are the same parameters, a stable insert diameter is not available in the submerged AWJT. It can be claimed that this value is constantly changing according to pressure and abrasive particle behavior. For this reason, only regression equations were used for reliability experiments in the study.

$$\%Error = |(Exp. - Pre.)/Exp| \times 100 \tag{6}$$

$$Ra = f^2/32.r \tag{7}$$

Table 6
Ranking for optimum points.

Exp. No	TOPSIS Method				VIKOR Method			
	S_i+	S_i-	C_i	Rank	ΣE_i	F_i	Q_i	Rank
1	0.054152	0.05008	0.480469	9	0.447311	0.268561	0.441877	19
2	0.048885	0.055484	0.531613	8	0.411278	0.242528	0.393017	20
3	0.044709	0.062409	0.582622	6	0.284532	0.227032	0.307851	22
4	0.04485	0.060066	0.572513	7	0.361668	0.224168	0.345672	21
5	0.041614	0.064729	0.608681	5	0.291759	0.210509	0.29287	23
6	0.033771	0.075643	0.691346	4	0.172064	0.172064	0.185306	24
7	0.024275	0.084805	0.777458	3	0.131169	0.123669	0.108373	25
8	0.016887	0.091713	0.844503	2	0.104709	0.085959	0.051305	26
9	**0.000169**	**0.10682**	**0.998418**	**1**	**0.06125**	**0.06125**	**0**	**27**
10	0.081872	0.022782	0.21769	18	0.737933	0.389183	0.734129	10
11	0.073512	0.030313	0.291959	17	0.589032	0.362782	0.624735	12
12	0.072898	0.031243	0.300003	16	0.662542	0.348792	0.647945	11
13	0.068754	0.035193	0.338566	15	0.624219	0.330469	0.606653	13
14	0.06654	0.037352	0.359529	14	0.542273	0.328523	0.560789	15
15	0.066107	0.037679	0.363046	13	0.562463	0.323713	0.566061	14
16	0.061276	0.043615	0.415815	12	0.446527	0.307777	0.48615	16
17	0.059093	0.045539	0.435234	11	0.448233	0.295733	0.473334	17
18	0.055186	0.048802	0.469305	10	0.473116	0.271866	0.459388	18
19	0.109414	0	0	27	1	0.5	1	1
20	0.105688	0.003726	0.034053	26	0.981016	0.5	0.989889	2
21	0.102939	0.004355	0.040587	25	0.925946	0.478446	0.935994	3
22	0.097755	0.006944	0.066322	23	0.820957	0.469707	0.870116	5
23	0.100045	0.006735	0.063073	24	0.899233	0.466733	0.908418	4
24	0.095517	0.01114	0.104448	22	0.873158	0.444408	0.869088	6
25	0.092434	0.012836	0.12193	21	0.816732	0.437982	0.831711	7
26	0.089836	0.015184	0.144582	20	0.794173	0.426673	0.806807	8
27	0.08648	0.018242	0.174192	19	0.764558	0.412058	0.77438	9

Table 7
Results of confirmation experiments and predicted values by regression equations.

Parameter	Point	For regression analysis		
		Experimental	Predicted	Error (%)
R_a	Optimum (TS: 40 mm/min, AFR: 310 g/min, SS: 300 rpm)	1.95	1.695	13.07
	Random (TS: 140 mm/min, AFR: 210 g/min, SS: 200 rpm)	3.17	3.495	10.25
	Random (TS: 240 mm/min, AFR: 110 g/min, SS: 300 rpm)	5.04	5.095	1.09
MRR	Optimum (TS: 40 mm/min, AFR: 310 g/min, SS: 300 rpm)	200.93	183.88	8.49
	Random (TS: 140 mm/min, AFR: 210 g/min, SS: 200 rpm)	127.46	128.48	0.80
	Random (TS: 240 mm/min, AFR: 110 g/min, SS: 300 rpm)	85.63	81.68	4.61

4. Conclusions

In this study, it is aimed to improve the machinability of castamide material by using submerged AWJT process. The results are as follows:

1. The noise level, which was 108.8 dB under conventional AWJT conditions, was reduced to 86.1 dB with submerged AWJT system. In addition, a stable machining zone was formed by eliminating splash.
2. Under conventional AWJT conditions, the lowest Ra value was 1.73 μm and the maximum *MRR* value was 212 mm^3/min. And for the submerged AWJT conditions, the lowest R_a value was 1.46 μm, the maximum MRR value was 200.93 mm^3/min.
3. According to the ANOVA results TS, AFR and SS parameters affect the R_a value by 83.11%, 1.10% and 0.53%, respectively. R_a was mainly affected by TS and its value increased with increasing TS parameter. Additionally, TS, AFR and SS parameters were found to affect *MRR* value by 85.56%, 10.26% and 1.10%, respectively. *MRR* values decreased with increasing TS and increased with increasing AFR parameter.
4. The ANOVA results of the conventional AWJT and the submerged AWJT processes are similar.
5. R-Sq values obtained by analysis of variance were determined as 91.32% and 99.89% for R_a and *MRR* values, respectively. The obtained values are statistically sufficient.
6. Optimum test conditions according to TOPSIS and VIKOR methods were determined as TS: 40 mm/min, AFR: 310 g / min, SS: 300 rpm.
7. As a result of validation tests for optimization of TOPSIS and regression equations, error rates below 20% was achieved which ensures the reliability of the experimental design.

Declaration of Competing Interest

The authors declare that they have no known competing financial interests or personal relationships that could have appeared to influence the work reported in this paper.

References

[1] I. Karakurt, G. Aydin, K. Aydiner, Analysis of the kerf angle of the granite machined by abrasive waterjet (AWJ), Ind. J. Eng. Mater. Sci. 18 (2011) 435–442.
[2] L.M. Hlaváč, I.M. Hlaváčová, V. Geryk, Š. Plančár, Investigation of the taper of kerfs cut in steels by AWJ, Int. J. Adv. Manuf. Technol. 77 (2015) 1811–1818, https://doi.org/10.1007/s00170-014-6578-9.
[3] G. Aydin, I. Karakurt, K. Aydiner, Prediction of the cut depth of granitic rocks machined by abrasive waterjet (AWJ), Rock Mech. Rock Eng. 46 (2013) 1223–1235, https://doi.org/10.1007/s00603-012-0307-1.
[4] G. Aydin, I. Karakurt, K. Aydiner, An investigation on surface roughness of granite machined by abrasive waterjet, Bull. Mater. Sci. 34 (2011) 985–992, https://doi.org/10.1007/s12034-011-0226-x.
[5] I. Karakurt, G. Aydin, K. Aydiner, A machinability study of granite using abrasive waterjet cutting technology, Gazi Univ. J. Sci. 24 (2011) 143–151.
[6] B. Strnadel, L.M. Hlaváč, L. Gembalová, Effect of steel structure on the declination angle in AWJ cutting, Int. J. Mach. Tools Manuf 64 (2013) 12–19, https://doi.org/10.1016/j.ijmachtools.2012.07.015.
[7] I. Karakurt, G. Aydin, K. Aydiner, An investigation on the kerf width in abrasive waterjet cutting of granitic rocks, Arabian J. Geosci. 7 (2014) 2923–2932, https://doi.org/10.1007/s12517-013-0984-4.
[8] L.M. Hlaváč, L. Gembalová, P. Štěpán, I.M. Hlaváčová, Improvement of abrasive water jet machining accuracy for titanium and TiNb alloy, Int. J. Adv. Manuf. Technol. 80 (2015) 1733–1740, https://doi.org/10.1007/s00170-015-7132-0.
[9] I. Karakurt, G. Aydin, K. Aydiner, An experimental study on the depth of cut of granite in abrasive waterjet cutting, Mater. Manuf. Process. 27 (2012) 538–544, https://doi.org/10.1080/10426914.2011.593231.
[10] L.M. Hlavac, S. Spadło, D. Krajcarz, I.M. Hlavacova, Influence traverse speed on surface quality after water-jet cutting for hardox steel, in: METAL 2015–24th International Conference on Metallurgy and Materials, Conference Proceedings, 2015, pp. 723–728.
[11] P. Gudimetla, J. Wang, W. Wong, Kerf formation analysis in the abrasive waterjet cutting of industrial ceramics, J. Mater. Process. Technol. 128 (2002) 123–129, https://doi.org/10.1016/S0924-0136(02)00437-5.
[12] L.M. Hlaváč, D. Krajcarz, I.M. Hlaváčová, S. Spadło, Precision comparison of analytical and statistical-regression models for AWJ cutting, Precis. Eng. 50 (2017) 148–159, https://doi.org/10.1016/j.precisioneng.2017.05.002.
[13] L.M. Hlaváč, I.M. Hlaváčová, L. Gembalová, J. Kaličinský, S. Fabian, J. Měšťánek, J. Kmec, V. Mádr, Experimental method for the investigation of the abrasive water jet cutting quality, J. Mater. Process. Technol. 209 (2009) 6190–6195, https://doi.org/10.1016/j.jmatprotec.2009.04.011.
[14] L.M. Hlaváč, R. Kocich, L. Gembalová, P. Jonšta, I.M. Hlaváčová, AWJ cutting of copper processed by ECAP, Int. J. Adv. Manuf. Technol. 86 (2016) 885–894, https://doi.org/10.1007/s00170-015-8236-2.
[15] M.C.P. Selvan, N.M.S. Raju, R. Rajavel, Effects of process parameters on depth of cut in abrasive waterjet cutting of cast iron, Int. J. Sci. Eng. Res. 2 (2011) 1–5.
[16] I. Karakurt, G. Aydin, K. Aydiner, A study on the prediction of kerf angle in abrasive waterjet machining of rocks, Proc. Inst. Mech. Eng., Part B: J. Eng. Manuf. 226 (2012) 1489–1499, https://doi.org/10.1177/0954405412454395.
[17] H. Takeyama, N. Lijima, Machinability of glassfiber reinforced plastics and application of ultrasonic machining, Ann. CIRP. 37 (1988) 93–96, https://doi.org/10.17951/pjss/2017.50.2.155.
[18] K. Weinert, C. Kempmann, Cutting temperatures and their effects on the machining behaviour in drilling reinforced plastic composites, Adv. Eng. Mater. 6 (2004) 684–689, https://doi.org/10.1002/adem.200400025.
[19] W. König, P. Grass, Quality definition and assessment in drilling of fibre reinforced thermosets, CIRP Ann. 38 (1989) 119–124.
[20] W.C. Chen, Some experimental investigations in the drilling of carbon fiber-reinforced plastic (CFRP) composite laminates, Int. J. Mach. Tools Manuf. 37 (1997) 1097–1108, https://doi.org/10.1016/S0890-6955(96)00095-8.
[21] J. Kechagias, G. Petropoulos, V. Iakovakis, S. Maropoulos, An investigation of surface texture parameters during turning of a reinforced polymer composite using design of experiments and analysis, Int. J. Exp. Design Process Optimisat. 1 (2009) 164, https://doi.org/10.1504/ijedpo.2009.030317.
[22] J.B. Zimmerman, Formulation Evaluation of Emulsifier Systems For Petroleumand Bio-Based Semi-Synthetic Metalworking Fluids, University of Michigan, 2003.
[23] W.F. Sales, A.E. Diniz, Á.R. Machado, Application of cutting fluids in machining processes, J. Brazilian Soc. Mech. Sci. 23 (2001).
[24] E. Yücel, M. Günay, M. Ayyıldız, Ö. Erkan, F. Kara, Talaşlı İmalatta Kullanılan Kesme Sıvılarının İnsan Sağlığına Etkileri Ve Sürdürülebilir Kullanımı, in: 6th International Advanced Technologies Symposium (IATS'11), Elazığ, Turkey, 2011: pp. 116–121.
[25] D.S. Pillay, N.A.C. Sidik, Tribological properties of biodegradable nano-lubricant, J. Adv. Res. Fluid Mech. Thermal Sci. 33 (2017) 1–13.
[26] T. Mang, W. Dresel, eds., Lubricants and Lubrication, Weinheim, Germany, 2007. doi:10.1002/1521-3773(20011015)40:20<3919::aid-anie3919>3.0.co;2-m.
[27] H. Liu, J. Wang, N. Kelson, R.J. Brown, A study of abrasive waterjet characteristics by CFD simulation, J. Mater. Process. Technol. 153–154 (2004) 488–493, https://doi.org/10.1016/j.jmatprotec.2004.04.037.
[28] C. Ma, R.T. Deam, A correlation for predicting the kerf profile from abrasive water jet cutting, Exp. Therm. Fluid Sci. 30 (2006) 337–343, https://doi.org/10.1016/j.expthermflusci.2005.08.003.
[29] U. Andersson, G. Holmqvist, Abrasive Waterjet Used As a Tool for Producing Materials, Test Specimens (2003).

[30] A.W. Momber, R. Kovacevic, Principles of Abrasive Water Jet Machining, Springer Science & Business Media, 2012.
[31] F. Kartal, M.H. Çetin, H. Gökkaya, Z. Yerlikaya, Optimization of abrasive water jet turning parameters for machining of low density polyethylene material based on experimental design method, Int. Polym. Proc. 29 (2014) 535–544, https://doi.org/10.3139/217.2925.
[32] F. Kartal, Z. Yerlikaya, Investigation of surface roughness and MRR for engineering polymers with the abrasive water jet turning process, Int. Polym. Proc. 31 (2016) 336–345, https://doi.org/10.3139/217.3185.
[33] K. Kumar, D. Zindani, J.P. Davim, Adv. Mach. Manuf. Process. (2018), https://doi.org/10.1007/978-3-319-76075-9.
[34] D.K. Kalla, B. Zhang, R. Asmatulu, P.S. Dhanasekaran, Current research trends in abrasive waterjet machining of fiber reinforced composites, Mater. Sci. Forum 713 (2012) 37–42, https://doi.org/10.4028/www.scientific.net/MSF.713.37.
[35] A. Radvanská, T. Ergić, Ž. Ivandić, S. Hloch, J. Valicek, J. Mullerova, Technical possibilities of noise reduction in material cutting by abrasive water-jet, Strojarstvo. 51 (2009) 347–354.
[36] M. Bozdemir, S. Aykut, Optimization of surface roughness in end milling Castamide, Int. J. Adv. Manuf. Technol. 62 (2012) 495–503, https://doi.org/10.1007/s00170-011-3840-2.
[37] L.M. Hlaváč, P. Palička, Testing of parameters for turning by abrasive water jets, In Proceedings of the 18th International Conference on Water Jetting, Gdansk, Poland, n.d.: pp. 123–128.
[38] M.H. Cetin, B. Ozcelik, E. Kuram, E. Demirbas, Evaluation of vegetable based cutting fluids with extreme pressure and cutting parameters in turning of AISI 304L by Taguchi method, J. Cleaner Prod. 19 (2011) 2049–2056, https://doi.org/10.1016/j.jclepro.2011.07.013.
[39] G.T. Alvali, Application of Engineering and Economy Approaches to the Transport Technology: A Case Study of Freight Wagon Bogie, Karabuk University, 2019.
[40] M. Jahan, A., Edwards, K., L. and Bahraminasab, Multi-criteria Decision Analysis, For Supporting the Selection of Engineering Materials in Product Design, Second Edi, USA, 2013.
[41] C.-L. Hwang, K. Yoon, Multiple Attribute Decision Making Methods and Applications, Springer, New York, 1981.
[42] M. Hashish, D.E. Steele, D.H. Bothell, Machining with super-pressure (690 MPa) waterjets, Int. J. Mach. Tools Manuf. 37 (1997) 465–479, https://doi.org/10.1016/S0890-6955(96)00016-8.
[43] A.I. Ansari, M. Hashish, M.M. Ohadi, Flow visualization study of the macromechanics of abrasive-waterjet turning, Exp. Mech. 32 (1992) 358–364, https://doi.org/10.1007/BF02325589.
[44] S.R. Lohar, P.R. Kubade, Investigation of effect of abrasive water jet machining (AWJM) process parameters on performance characteristics of high carbon high chromium steel (AISI D3), IARJSET. 4 (2017) 152–158, https://doi.org/10.17148/iarjset/ncdmete.2017.35.
[45] M. Hashish, Macro Characteristics of AWJ Turned Surfaces", Proceedings of the WJTA. 1 (2001) 45–58.
[46] D.C. Montgomery, Design and Analysis of Experiments, Wiley, New York, USA, 2004.
[47] J. Wang, Abrasive waterjet machining of polymer matrix composites – Cutting performance, erosive process and predictive models, Int. J. Adv. Manuf. Technol. 15 (1999) 757–768.
[48] U. Çaydaş, A. Hasçalik, A study on surface roughness in abrasive waterjet machining process using artificial neural networks and regression analysis method, J. Mater. Process. Technol. 202 (2008) 574–582, https://doi.org/10.1016/j.jmatprotec.2007.10.024.
[49] J. Valíček, S. Hloch, D. Kozak, Surface geometric parameters proposal for the advanced control of abrasive waterjet technology, Int. J. Adv. Manuf. Technol. 41 (2009) 323–328, https://doi.org/10.1007/s00170-008-1489-2.
[50] S. Hloch, S. Fabian, L. Straka, Factor analysis and mathematical modelling of AWJ cutting, Proceedings of the International Conference of DAAAM Baltic . (2006) 127–132.
[51] V. Gupta, P.M. Pandey, M.P. Garg, R. Khanna, N.K. Batra, Minimization of kerf taper angle and kerf width using Taguchi's method in abrasive water jet machining of marble, Procedia Mater. Sci. 6 (2014) 140–149, https://doi.org/10.1016/j.mspro.2014.07.017.
[52] G. Aydin, I. Karakurt, C. Hamzacebi, Artificial neural network and regression models for performance prediction of abrasive waterjet in rock cutting, Int. J. Adv. Manuf. Technol. 75 (2014) 1321–1330, https://doi.org/10.1007/s00170-014-6211-y.
[53] S. Hloch, M. Gombár, S. Fabian, L. Straka, Factor analysis of abrasive waterjet process factors influencing the cast aluminum surface roughness, Manuf. Sci. Technol. (2006) 145–149.
[54] R. Manu, N.R. Babu, An erosion-based model for abrasive waterjet turning of ductile materials, Wear 266 (2009) 1091–1097, https://doi.org/10.1016/j.wear.2009.02.008.
[55] L.M. Hlaváč, B. Strnadel, J. Kaličinský, L. Gembalová, The model of product distortion in AWJ cutting, Int. J. Adv. Manuf. Technol. 62 (2012) 157–166, https://doi.org/10.1007/s00170-011-3788-2.
[56] L.M. Hlaváč, I.M. Hlaváčová, V. Geryk, Taper of kerfs made in rocks by abrasive water jet (AWJ), Int. J. Adv. Manuf. Technol. 88 (2017) 443–449, https://doi.org/10.1007/s00170-016-8782-2.